Science Advances
AAAS

advances.sciencemag.org/cgi/content/full/6/2/eaav3400/DC1

Supplementary Materials for

Silica gel solid nanocomposite electrolytes with interfacial conductivity promotion exceeding the bulk Li-ion conductivity of the ionic liquid electrolyte filler

Xubin Chen, Brecht Put, Akihiko Sagara, Knut Gandrud, Mitsuhiro Murata, Julian A. Steele, Hiroki Yabe, Thomas Hantschel, Maarten Roeffaers, Morio Tomiyama, Hidekazu Arase, Yukihiro Kaneko, Mikinari Shimada, Maarten Mees, Philippe M. Vereecken*

*Corresponding author. Email: vereeck@imec.be

Published 10 January 2020, *Sci. Adv.* **6**, eaav3400 (2020)
DOI: 10.1126/sciadv.aav3400

This PDF file includes:

Supplementary Materials

Table S1. Structural properties of silica matrix in the nano-SCE for increasing molar fraction of ionic liquid to silica (*x* value) determined from N_2 adsorption/desorption or BET measurements and TEM observations. The water content was determined from the excess weight difference from non-volatile compounds. The density of the vacuum dried nano-SCE was obtained from Pycnometer measurements.

x-value	Theoretical Weight percentage Silica in SCE (wt. %)	Theoretical volume percent of ILE in SCE (vol. %)	Density SCE (g/cm^3)	Excess mass (wt. %)	BET surface area (mesopores and macropores) (m^2/g silica)	TEM surface area micropores (m^2/g silica)	Equivalent number of adsorbed ice water layers (BET area)	Equivalent number of adsorbed ice water layers (total area)	Equivalent thickness ILE layer (nm)*	Pore size from BET measurement (nm)	Equivalent SiO_2 sheet thickness** (nm)	Silica nanoparticle size from TEM (nm)
x=0.5	18.8	81	1.53	3.0	808	650	0.4	0.0	3.6	7.0	2.2	7.5
x=0.75	13.4	86	-	3.9	(900)	(525)	(0.9)	(0.5)	(4.8)	-	(2.4)	-
x=1	10.4	90	1.51	7.9	1048	400	2.7	1.8	5.5	10	2.7	12
x=1.5	7.2	93	1.50	7.6	908	360	4.6	2.9	9.5	16	2.3	13.5
x=1.75	6.2	94	1.51	7.7	(1000)	(355)	(4.9)	(3.5)	(10.1)	-	(2.4)	-
x=2	5.5	95	1.47	9.8	1005	(350)	(7.3)	(5.3)	(11.5)	11	(2.4)	-

* Assuming a flat silica surface; ** Assuming a layered structure

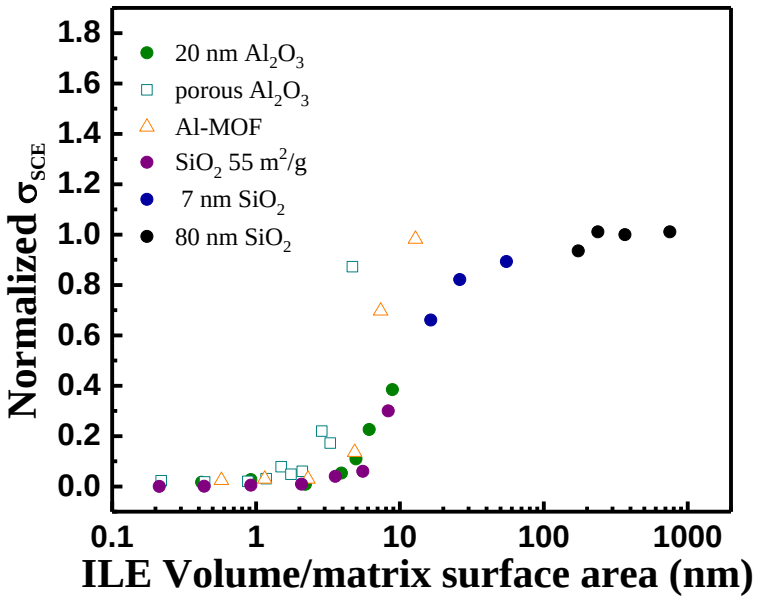

Fig. S1. Normalized conductivity versus equivalent ILE thickness. (ratio of ILE volume/surface area of the silica matrix) for particle-SCEs with ILE with different format particle matrices: 20 nm Al_2O_3 (green circles), porous Al_2O_3 microparticles (blue open squares, own work), MIL-100(Al) micropoarticles (orange open triangles, own work), SiO_2 with surface area of 55 m^2/g (purple circles) (*46*), 7 nm SiO_2 nanoparticles (blue circles) (*47*), 80 nm SiO_2 nanoparticles (black circles) (*48*).

Figure S1 compiles results from literature and from own work for solid composite electrolytes (SCE) with ionic liquid electrolyte as filler. The SCE were made from solid oxide nanoparticles, mesoporous microparticles of silica, alumina and an alumina-based Metal Organic Framework (MOF). So far, all particle-based ILE-SCE did not show any enhancement of the conductivity compared to the pure ILE reference. The conductivity of our sol-gel derived SCE on the other hand exceeds that of the corresponding ILE.

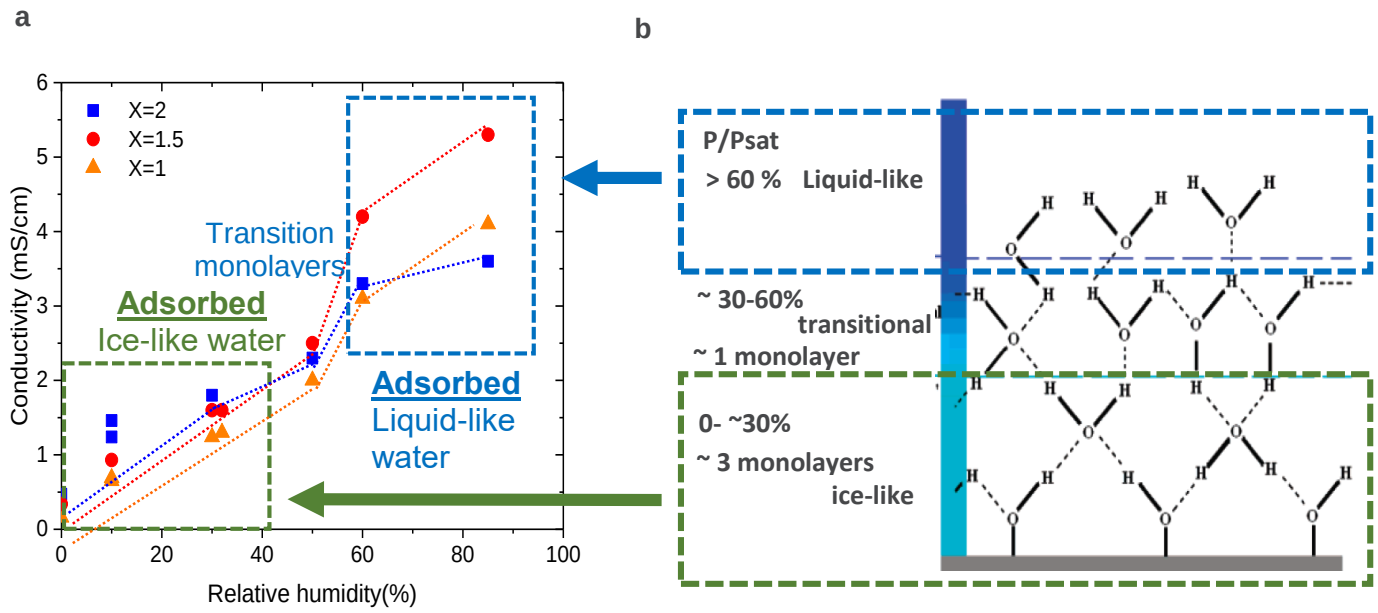

Fig. S2. The effect of ice-like and liquid-like adsorbed water on nano-SCE ion conductivity. (**a**) conductivity of nano-SCE with x-value of 2 (blue squares), 1.5 (red circles), and 1 (orange triangles) exposed to different relative humidity in a N_2 box; (**b**) a schematic of the water layers absorbed on silanol terminated silica at different relative humidity; adapted from ref. (*35*). For planar silica, up to three monolayers of ice water are formed in the range of 0-30% RH. A fourth monolayer of transitional water is formed between 30-60% and finally adsorbed liquid water is formed at RH >60%, according to ref.(*35*)

a

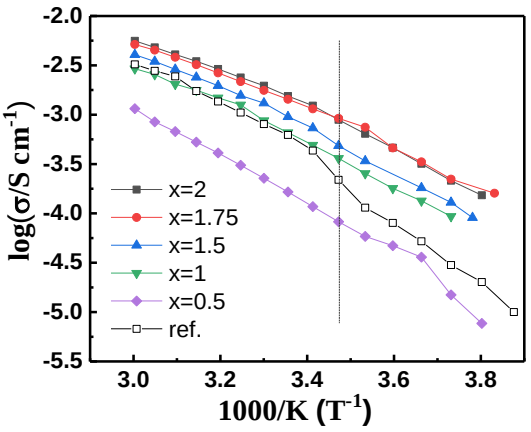

b

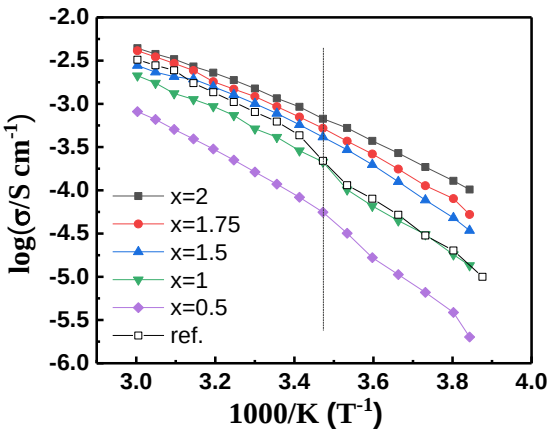

c

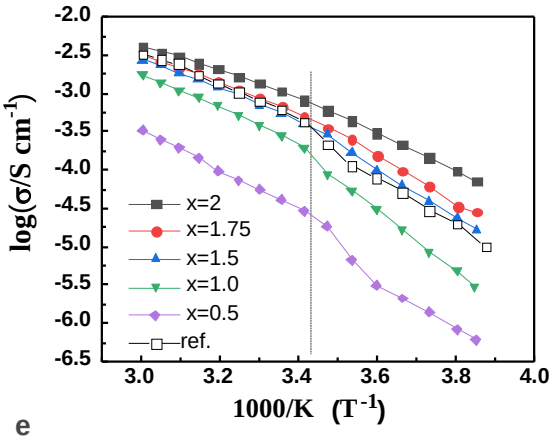

d

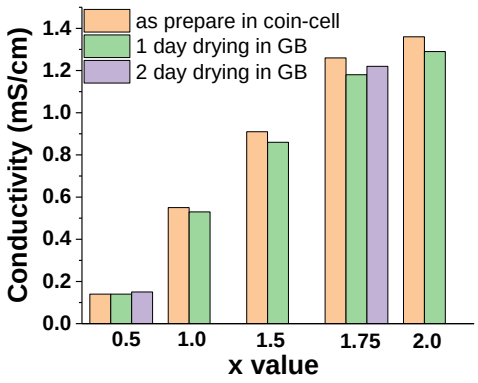

e

sample	Day 2		Day 8		Day 20	
	Ea1 (eV)	Ea2 (eV)	Ea1 (eV)	Ea2 (eV)	Ea1 (eV)	Ea2 (eV)
X=2	0.34±0.01	0.49±0.01	0.39±0.01	0.53±0.01	0.38±0.01	0.50±0.01
X=1.75	0.35±0.01	0.47±0.03	0.39±0.01	0.53±0.01	0.43±0.01	0.63±0.02
X=1.5	0.38±0.01	0.48±0.02	0.37±0.01	0.60±0.02	0.44±0.01	0.64±0.01
X=1	0.36±0.02	0.47±0.01	0.45±0.01	0.58±0.01	0.48±0.01	0.80±0.01
X=0.5	0.50±0.01	0.63±0.07	0.54±0.01	0.73±0.06	0.55±0.01	0.65±0.04
ILE ref.	0.46±0.01	0.65±0.02				

Fig. S3. Temperature dependence of the conductivity of the nano-SCE. Temperature dependence of the nano-SCE with x value of 2 (black squares), 1.75 (red circles), 1.5(blue triangles), 1.0 (green triangles), 0.5 (purple diamonds) and ILE ref. (open black squares), additionally dried in a glovebox with relative humidity of 0.0005% for (**a**) 2 days, (**b**) 8 days and (**c**) 20 days; (**d**) the conductivity of a nano-SCE as-sealed in a coin cell used for the temperature dependence measurements (orange), and of the coin cell in the glovebox for 1 day (green) and 2 days (purple) showing the conductivity is stable when sealed; (**e**) activation energy of the nano-SCE with ice water content equivalent with 2, 8 and 20 days of drying in the glovebox (see also Figure 3c in main text).

The conductivity of the nano-SCE with x values >1 shows a smooth continuous trend with decreasing temperature. On the contrary, two distinct regions are observed in the temperature dependence plots for the nano-SCE with low x values and for the ILE ref., as indicated by the dotted lines on fig. S3 a, b, c. Two activation energies Ea1, and Ea2 at high and low temperature regions can be respectively extracted. As listed in the table in panel e, the activation of the nano-SCE with high x-values are lower than those of the ILE reference, indicating the presence of interfacial conduction in the nanocomposite. Figure S3d shows the stability of the SCE conductivity measured in the coin cell, demonstrating that the coin cell is well sealed for such temperature dependence measurements.

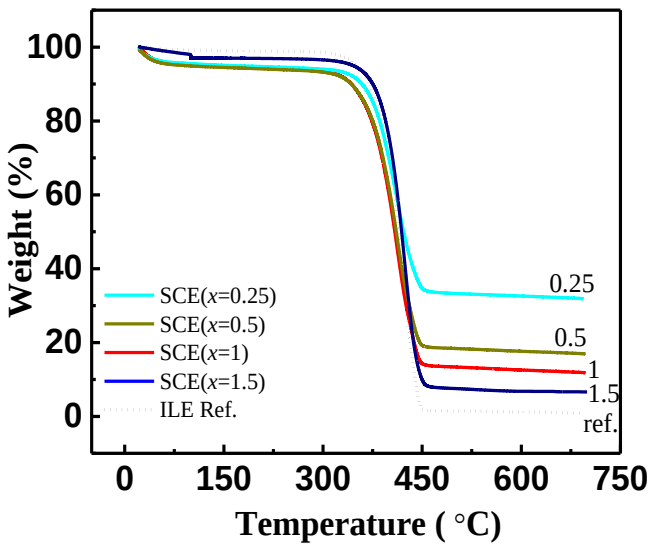

Fig. S4. TGA curves for nano-SCE. TGA curves for nano-SCE with x value of 0.25 (light blue), 0.5 (green), 1 (red), 1.5(blue), and for the ILE reference (dotted line). The heating rate was 2 °C/min and the ambient was N_2. During sample preparation, the samples were exposed to air.

On the TGA curves, the initial weight loss below 60 °C corresponds to the loss of the excess water introduced during the sample preparation, in which the samples were exposed to the air. The ILE starts to decompose at about 390 °C. The decomposition products of the ILE are gaseous, as no weight was recorded after the decomposition of ILE reference. The nano-SCEs also start to lose weight at about 390 °C, corresponding to the decomposition of the ILE inside the samples. The weight after the decomposition corresponds to the remaining silica and fits very well with what is expected from ILE to silica (TEOS) ratio as mixed in the sol-gel precursor solution.

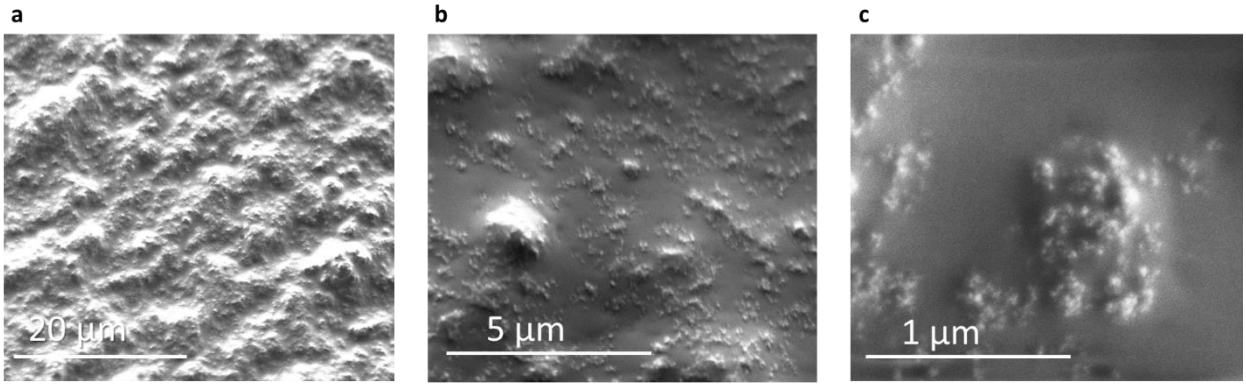

Fig. S5. SEM images of the nano-SCE. SEM images showing the SCE without the removal of the ILE, with increasing magnification going from **a** to **c**. The nano-SCE showed no clear microstructure in the SEM except for a smooth surface with some silica patches peeking out. These patches range from 100 nm up to 1.5 µm in diameter.

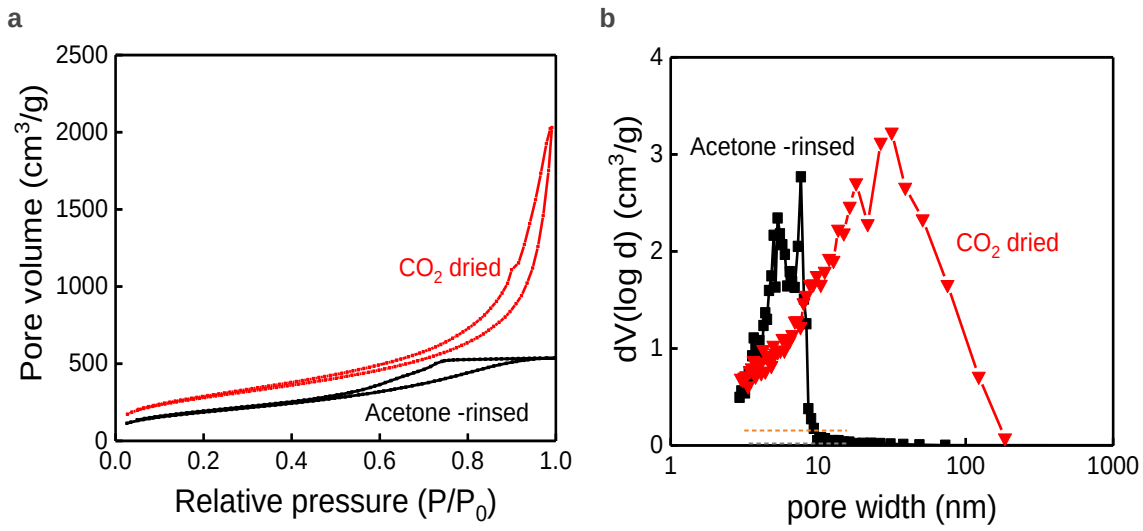

Fig. S6. N_2 adsorption/desorption isotherm of the silica derived from nano-SCE. N_2 adsorption/desorption isotherm (**a**) and pore size distribution (**b**) of the porous silica matrix derived from a nano-SCE (x=1.5) pellet by rising with ethanol and CO_2 supercritical drying (red), and by rinsing out the ILE with acetone and air drying (black); BJH method is used for calculation of the pore size, with an assumption that the pores in the silica are cylindric.

The isotherms show hysteresis between the adsorption and desorption branches, indicating the presence of mesopores in silica. The silica matrix derived after acetone rinsing has significantly lower pore volume compared to the one obtained by CO_2 super critical drying, due to partial collapse of the porous structure in the former treatment.

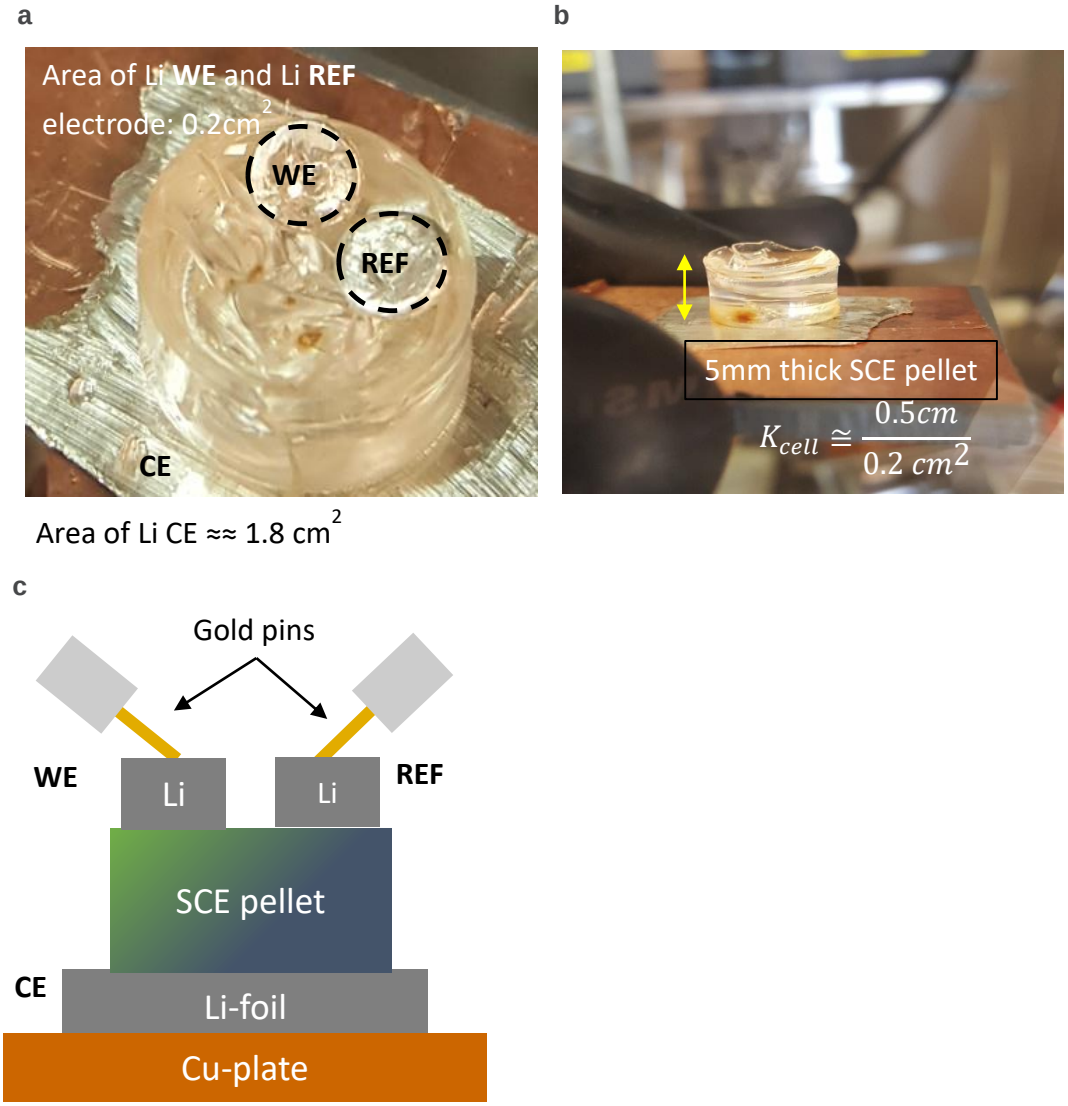

Fig. S7. Solid-state three-electrode setup for cyclic voltammetry on nano-SCE pellets. (**a**, **b**) image of the setup where the nano-SCE pellet (~5 mm in diameter) is placed on a large Li foil as counter electrode (CE, area 1.8 cm^2), and two smaller Li disks are pressed on the top of the nano-SCE pellet as working and reference electrode (WE, RE, area 0.2 cm^2); the nano-SCE is thick enough so that the cell constant (0.5 cm/ 0.2 mm^2 in this case) can be determined by using the area of working electrode; the area of the counter electrode is about 10 times that of the working electrode; (**c**) a schematic showing the electrical contact of the setup. (Photo Credit: Knut Gandrud, imec.)

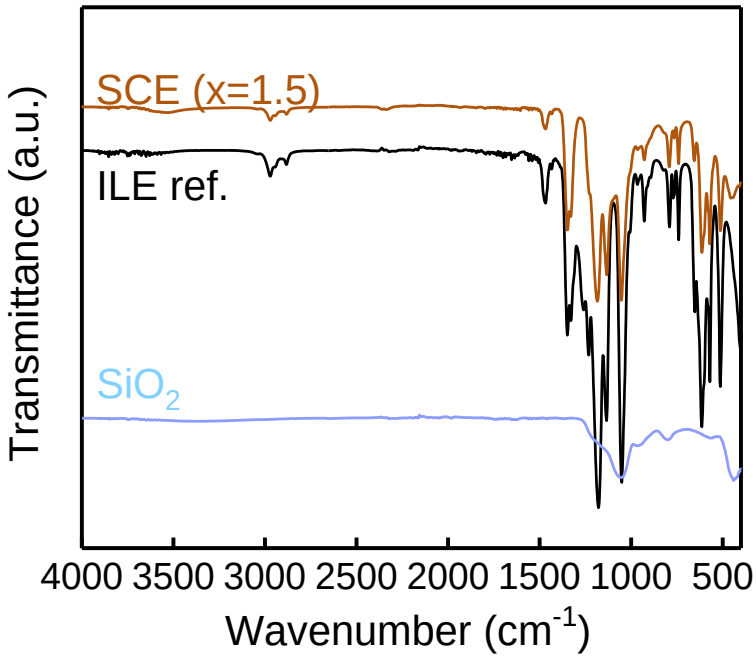

Fig. S8. IR spectra of nano-SCE (*x* = 1.5), ILE, and silica in the range of 4000 to 400 cm^{-1}.

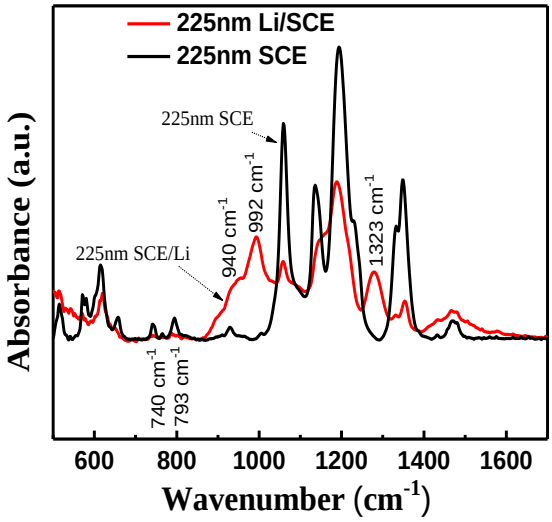

Fig. S9. IR spectra of 225-nm nano-SCE (x = 1.5) and Li/SCE thin-film stack.

The nano-SCE thin film and the lithium was deposited by spin-coating and thermal evaporation respectively. As can be seen on the spectrum of the stack, the vibration peaks of the cation at 740 cm^{-1} and 793 cm^{-1} were absent, but the vibration peaks of vinyl and amine groups at 940 cm^{-1}, 994 cm^{-1} and 1323 cm^{-1} were present. The results show that the cation rings are opened due to the reaction with lithium.